Thermochimica Acta 491 (2009) 103–108

Contents lists available at ScienceDirect

Thermochimica Acta

journal homepage: www.elsevier.com/locate/tca

Thermal degradation behavior of hydrogenated nitrile-butadiene rubber (HNBR)/clay nanocomposite and HNBR/clay/carbon nanotubes nanocomposites

Shuguo Chen, Haiyang Yu, Wentan Ren, Yong Zhang*

State Key Laboratory of Metal Matrix Composites, School of Chemistry and Chemical Technology, Shanghai Jiao Tong University, Shanghai 200240, China

ARTICLE INFO

Article history:
Received 24 January 2009
Received in revised form 10 March 2009
Accepted 11 March 2009
Available online 24 March 2009

Keywords:
HNBR
Clay
Carbon nanotubes
Thermal degradation
Kinetics

ABSTRACT

The thermal degradation of hydrogenated nitrile-butadiene rubber (HNBR)/clay and HNBR/clay/carbon nanotubes (CNTs) nanocomposites was investigated with thermogravimetric analysis (TGA) by using Kissinger method, Flynn–Wall–Ozawa method and Friedman method. The activation energy sequence of HNBR and its nanocomposites is HNBR/clay/CNTs > HNBR/clay > HNBR. HNBR/clay/CNTs nanocomposites had higher char yield at 600 °C than HNBR/clay, which was attributed to the interaction of network between clay and CNTs. The activation energies of HNBR and HNBR nanocomposites had a sharply increase in the low conversion degree area and a slow increase in the high conversion degree area. The gases involved during thermal degradation in nitrogen atmosphere were studied by Fourier transform infrared spectroscopy coupled with TGA. The HNBR/clay/CNTs nanocomposites had lower thermal degradation rate than HNBR/clay, which could be attributed to that the clay-CNTs filler network reduced the diffusion speed of degradation products. The coexistence of clay and CNTs could form compact char layers with better barrier property than clay and thus improved the thermal stability of HNBR.

1. Introduction

Hydrogenated nitrile-butadiene rubber (HNBR) with excellent oil and hot-air ageing resistance has been extensively used in industry, such as automobile and petroleum extraction [1–5], especially at elevated temperatures. Thermal degradation kinetic parameters are important information for understanding polymer thermal degradation process at elevated temperatures [6], thus it is necessary to pay attention on the thermal degradation of HNBR nanocomposites. Nanoparticles have been demonstrated to improve the thermal stability of polymer [7–11]. Carbon nanotubes (CNTs) are a kind of ideal filler for polymer nanocomposites due to their superior thermal, mechanical and electrical properties [12,13]. CNTs could form a protective layer acting as a heat shield when they are well dispersed in polymer [14] and act as a radical scavenger and thus reduce the thermal decomposition of HNBR [15]. Organoclay is a kind of commonly used nanoscale filler for polymers due to its excellent mechanical properties, barrier property, and thermal stability. Thermal stability of polymer/clay nanocomposites has been studied [16–18]. Huang et al. [19] found that organoclay could greatly improve the thermal stability and aging resistance of HNBR in different mediums at elevated temperatures. The synergistic effect between CNTs and organoclay, such as in flame retardancy in polymers was also investigated [20–23]. The synergistic mechanism was generally explained that the coexistence of clay and CNTs could enhance the clay-CNTs network structure [21,24], which can hinder the movement of polymer chains and thus improve flame retardancy.

It is known that flame retardancy of polymer nanocomposites not only depends on their thermal stability but also on their degradation rate, char-forming rate and char yield, which deserve a deep investigation. The synergistic effect of CNTs and clay on the thermal degradation of polymer materials, especially on rubber nanocomposites, however, was seldom reported. In this article, HNBR/clay/CNTs nanocomposites were prepared by shear mixing and the effect of CNTs and clay on the thermal degradation of HNBR was investigated in terms of thermogravimetric analysis (TGA). The kinetic parameters of thermal degradation such as apparent activation energy (E_a), pre-exponential factor (A), reaction order (n) could be calculated by using various methods such as Kissinger [25], Flynn–Wall–Ozawa [26] and Friedman methods [27]. The thermal degradation of polymer materials can be quantitatively described to reveal the thermal stability from the viewpoint of kinetics.

The basic assumption of the thermal kinetics is that the thermal degradation reaction can represent by Arrhenius equation, *i.e.*, for a simple reaction [28]:

$$A_{solid} \rightarrow B_{solid} + C_{gas}$$

The Arrhenius equation has the following formula:

$$k = Ae^{-E_a/RT} \quad (1)$$

* Corresponding author. Tel.: +86 21 54742671; fax: +86 21 54741297.
E-mail address: yong_zhang@sjtu.edu.cn (Y. Zhang).

0040-6031/$ – see front matter © 2009 Elsevier B.V. All rights reserved.
doi:10.1016/j.tca.2009.03.010

Its reaction rate $d\alpha/dt$ can be written as

$$\frac{d\alpha}{dt} = kf(\alpha) \quad (2)$$

t is reaction time (s). α is conversion degree = $(W_0 - W_t)/(W_0 - W_\infty)$ (W_0, W_t, W_∞, are the initial, actual and final weights of the sample in the TGA curves, respectively). $f(\alpha)$ depends on the specific degradation reaction mechanism. The combination of (1) and (2) gives the following equation:

$$\frac{d\alpha}{dt} = Af(\alpha)e^{-E_a/RT} \quad (3)$$

In the degradation, the temperature is dependent on the heating time, Therefore

$$\frac{d\alpha}{dt} = \frac{d\alpha}{dT}\frac{dT}{dt} = \beta\frac{d\alpha}{dT} \quad (4)$$

β is heating rate (K/min), the combination of (3) and (4) gives the following formula:

$$\frac{d\alpha}{dT} = \frac{A}{\beta}f(\alpha)e^{-E_a/RT} \quad (5)$$

Integration of both sides of above equation and rearrangement give

$$g(\alpha) = \int_0^\alpha \frac{d\alpha}{f(\alpha)} = \frac{A}{\beta}\int_0^T e^{-E_a/RT}dT = \frac{ART^2}{\beta E_a}\left(1 - \frac{2RT}{E_a}\right)e^{-E_a/RT} \quad (6)$$

$g(\alpha)$ is the integral function of α. For the different solid reaction mechanisms, $g(\alpha)$ has different expressions [29]. These expressions can be used to predict the solid reaction mechanism reflected by the TGA curves, which can be used to the thermal kinetics of the HNBR/clay/CNTs.

1.1. Kissinger method (differential method) [25]

The Kissinger method adopts the following equation:

$$\ln\left(\frac{\beta}{T_{max}^2}\right) = \ln\frac{AR}{E_a} + \ln[n(1-\alpha_{max})^{n-1}] - \frac{E_a}{RT_{max}} \quad (7)$$

T_{max} is the temperature at the inflection point of TGA curve and α_{max} is the conversion degree at the inflection point. Plot of $\ln(\beta/T_{max}^2)$ against $1/T_{max}$ produces a fitted straight line. The apparent activation energy E_a can be calculated by the slope of the straight line $(-E_a/R)$.

1.2. Flynn–Wall–Ozawa method (integration method) [26]

The Flynn–Wall–Ozawa method adopts the following equation:

$$\log\beta = -\frac{0.457E_a}{RT} + \left\{\log\left[\frac{AE_a}{Rg(\alpha)}\right] - 2.315\right\} \quad (8)$$

At a given α, plot of $\log\beta$ against $1/T$ produces a fitted straight line with a slope $(-0.457E_a/R)$. The E_a can be calculated from the slope. The E_a of this method is independent with thermal degradation reaction mechanism in advance.

1.3. Friedman method [27]

The Friedman method is both a single heating-rate method and a multiple heating-rate method. The multiple heating-rate Friedman method is based on a comparison of weight-loss, determined at different heating rates. This method utilizes the following natural logarithmic differential equation:

$$\ln\left(\frac{d\alpha}{dt}\right) = \ln\left(\beta\frac{d\alpha}{dT}\right) = \ln A + n\ln(1-\alpha) - \frac{E_a}{RT} \quad (9)$$

By plotting $\ln(d\alpha/dt)$ against $1/T$ for a constant α, E_a can be obtained from the slope of $-E_a/R$. The reaction order (n) can also be calculated from the slope of $\ln(1-\alpha)$ versus $1/T$ at a constant $d\alpha/dt$. Then, the $\ln A$ can be obtained from the derived E_a and n values according to Eq. (9).

2. Experimental

2.1. Materials

HNBR with 39 wt% acrylonitrile (ACN) (Mooney viscosity, ML_{1+4}, at 100 °C = 70) was kindly provided by Lanxess Chemical (Shanghai) Co., Ltd. Carboxylated multi-wall carbon nanotubes (CNTs) with 3 wt% carboxyl content and 10–20 nm outer diameter were made in Chengdu Organic Chemistry Co., Ltd. The clay with trade name DK2 was kindly supplied by the Zhejiang Fenghong Clay Co., Ltd. Dicumyl peroxide (DCP) with 97% purity was supplied by Shanghai Gaoqiao Petroleum Co., Ltd.

2.2. Preparation

All the samples were prepared on a two-roll mill. 100 phr HNBR, 5 phr clay, and 3.6 phr DCP and CNTs were mixed on the mill for 15 min. The obtained compounds were finally compression cured at 170 °C for 20 min under 10 MPa.

2.3. Characterization

Thermal degradation was performed with a Q5000 TGA analyzer (TA Inc., USA) by heating from 25 to 600 °C under a nitrogen atmosphere at heating rates of 5, 10, 20 and 30 °C/min, respectively.

The gases involved during thermal degradation at a nitrogen atmosphere were studied by Fourier transform infrared spectroscopy coupled with TGA (TGA-FTIR) from 30 °C to 800 °C at a heating rate 20 °C /min in a TG 209 F1 (Netzsch, Germany) coupled with a infrared spectrometer (Tensor 27, Bruker, Germany) equipped with a gas cell which was heated to 200 °C to avoid the condensation of the degradation products inside the transfer line and the gas cell.

3. Results and discussion

HNBR and its nanocomposites present only one thermal degradation step in the temperature range 100–600 °C (Fig. 1). The incorporation of clay and CNTs causes a shift of the initial mass loss towards higher temperature. As seen from the peak of the first derivative, the temperature at which HNBR degradation rate is the highest is 451.4 °C, for a heating rate of 5 °C/min, while a small shift to higher temperatures is observed with the incorporation of clay and CNTs. Both clay and CNTs rise the initial-decomposing temperature at the weight loss of 5 wt%, the final char residue of HNBR/clay (100/5) is 3.1 wt%, but the char residues of HNBR/clay/CNTs (100/5/0.4) and HNBR/clay/CNTs (100/5/0.8) are 4.1 and 4.7 wt%, respectively, indicating that the CNTs improve the thermal stability of HNBR/clay. Ma et al. [21] reported that the coexistence of clay and CNTs could improve the thermal stability of acrylonitrile–butadiene–styrene nanocomposites as clay and CNTs can form a more effective confine space, which may be responsible for the improved thermal stability of HNBR nanocomposites. The reaction mechanism of polymer decomposition is a very complex radical chain mechanism, including initiation reactions, propagation reactions and termination reactions. Fig. 1 shows the main degradation temperature region of materials is 350–550 °C, which can be the temperature range used for data treatment. In order to more thoroughly analyze the degradation mechanism of HNBR and the effect of the clay and CNTs, it is important to evaluate the kinetic parameters (E_a, n, A). The degradation for all samples was studied

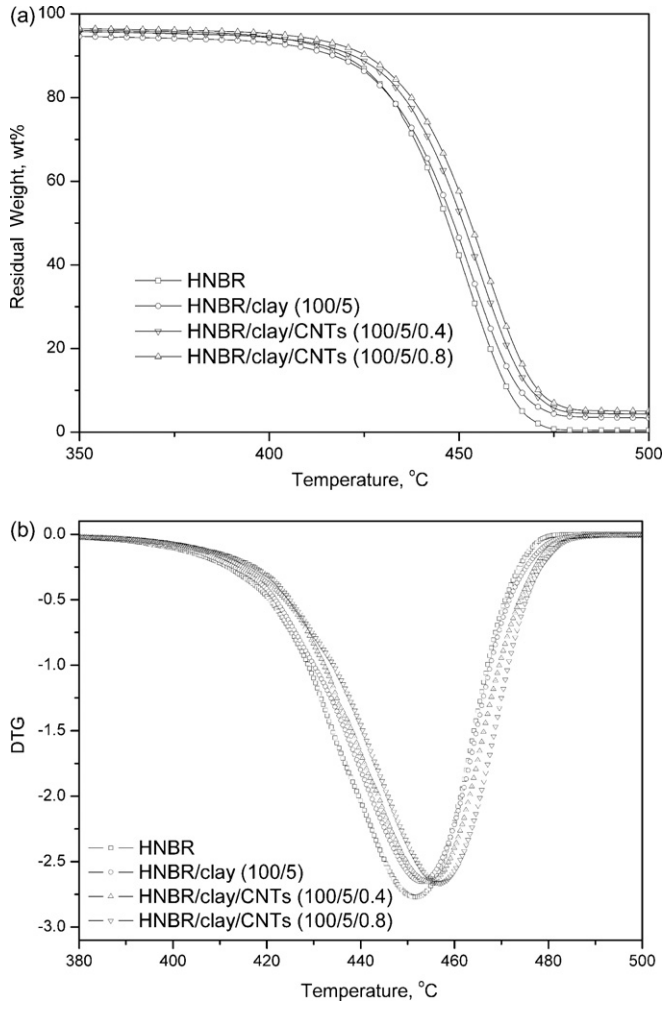

Fig. 1. TGA (a) and DTG (b) curves of different samples at a heating rate of 5 °C/min.

through non-isothermal measurements at different heating rates (5, 10, 20, 30 °C/min).

3.1. Kinetics analysis using Kissinger method [25]

Plots of $\ln(\beta/T_{max}^2)$ against $1/T_{max}$ show fitted straight lines with high linearly correlation coefficient (Fig. 2), showing the feasibility

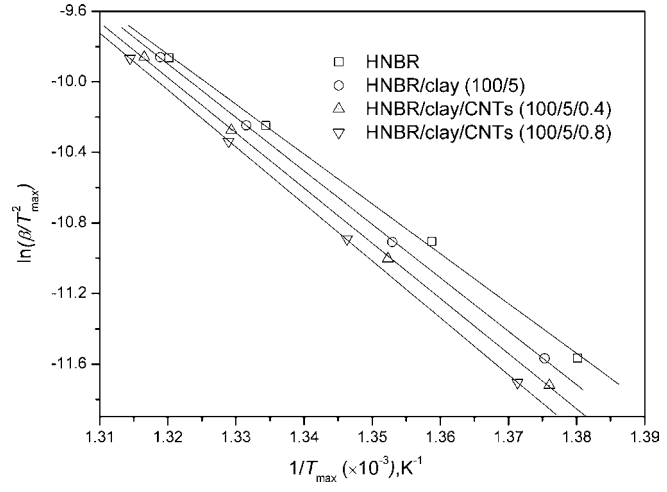

Fig. 2. Kissinger method applied to experimental TGA data at different heating rates.

Table 1
Inflection point temperature of TGA curves for nanocomposites at different heating rates.

Heating rate (°C/min)	$T_{inflection\ point}$ (°C) of HNBR/clay/CNTs			
	100/0/0	100/5/0	100/5/0.4	100/5/0.8
5	452	454	455	457
10	464	466	467	469
20	477	478	478	480
30	485	485	485	487

Table 2
The active energies (E_a) obtained using the Kissinger method for different samples.

	E_a (kJ/mol)	Rc^2
100/0/0	235	0.9989
100/5/0	252	0.9999
100/5/0.4	260	0.9998
100/5/0.8	268	0.9999

of Kissinger method. Since the fitted lines of different samples overlapped each other, the lines were parallel shifted on the X-direction. The inflection point temperatures of TGA curves of nanocomposites are included in Table 1. The E_a of thermal degradation of HNBR is 235 kJ/mol and the E_a of HNBR/clay, HNBR/clay/CNTs (100/5/0.4) and HNBR/clay/CNTs (100/5/0.8) increases to 252, 260 and 268 kJ/mol (Table 2), revealing that the clay and CNTs improve the thermal stability of HNBR. Especially small amount of CNTs increases the E_a by about 8 kJ/mol, indicating that the HNBR/clay/CNTs with higher char yield has higher E_a of thermal degradation, which can be ascribed to the better thermal stability of the char layer formed with good barrier property [30,31].

3.2. Kinetics analysis using Flynn–Wall–Ozawa method [26]

At a given conversion degree (α), plot of $\log\beta$ against $1/T$ produces a fitted straight line with a slope ($-0.457E_a/R$). The E_a can be calculated from the slope. The E_a of this method is independent of thermal degradation reaction mechanism in advance. The plot $1/T$ of against $\log\beta$ makes fitted straight lines with high linearly correlation coefficient (Rc^2) at different α (8–90%). The method utilizing the Doyle approximation is applicable if the straight lines fitted at different α (8–30%) parallel each other [26]. The fitted straight lines obtained at different α (8–90%) for HNBR nanocomposites are approximately parallel to each other and all the correlation coefficients are around 0.99, indicating the method is applicable to the HNBR nanocomposites. The E_a of HNBR and HNBR nanocomposites increases sharply at low α and becomes almost stable at α over 20% (Fig. 3), indicating a change in the rate limiting step of the degradation kinetics [7,32], caused by a shift of the rate limiting step from initiation to the degradation initiated by random scission. The average E_a of HNBR nanocomposites calculated from the Flynn–Wall–Ozawa method increases certainly with the incorporation of clay and CNTs (Table 3). The filler dependence of E_a for HNBR nanocomposites calculated by Flynn–Wall–Ozawa method is the same as that by Kissinger method, *i.e.* E_a increases when adding CNTs, indicating

Table 3
Activation energies of various samples obtained by Flynn–Wall–Ozawa method in α range 14%–90%.

HNBR/clay/CNTs	E_a (kJ/mol)
100/0/0	237
100/5/0	241
100/5/0.4	246
100/5/0.8	250

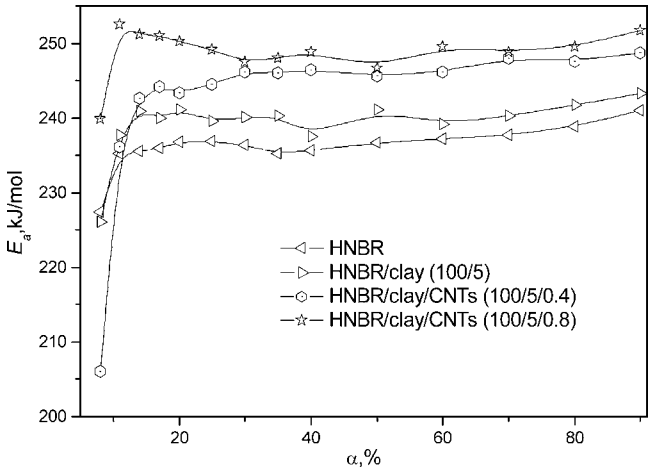

Fig. 3. Activation energies versus α obtained by Flynn–Wall–Ozawa method.

the two methods could be used in the HNBR/clay/CNTs system and the result is reliable, as Flynn–Wall–Ozawa and the Kissinger methods are model-free methods by using several different heating rates regardless the degradation model. The difference between Flynn–Wall–Ozawa method and Kissinger method is the treatment of TGA data at different heating rates and at a given α, which may cause the different E_a increase extent between Kissinger and Flynn–Wall–Ozawa methods [33].

3.3. Friedman method [26]

Friedman method can deal with the main degradation region of TGA curve of composites and calculate the E_a, n and A, while Kissinger and Flynn–Wall–Ozawa methods do not consider the solid phase reaction mechanism and both methods have some difficulty in calculating kinetic parameters such as n and A. The Friedman method was used by plotting $\ln(d\alpha/dt)$ versus $1/T$ for a constant α and, thus, the E_a was calculated (Fig. 4). The average of E_a, n and $\ln A$ are shown in Table 4. The dependence of E_a on α value presents the same tendency with Flynn–Wall–Ozawa method. The E_a increases sharply with the low α, while also has a significant decrease at $\alpha = 14\%$. After that, the E_a increases slightly with the increasing α, being almost stable. The independence of E_a on α indicates a complex reaction with the participation of at least of two mechanisms, which is rather typical phenomenon for many polymer [32]. The first mechanism corresponds to the part where small mass

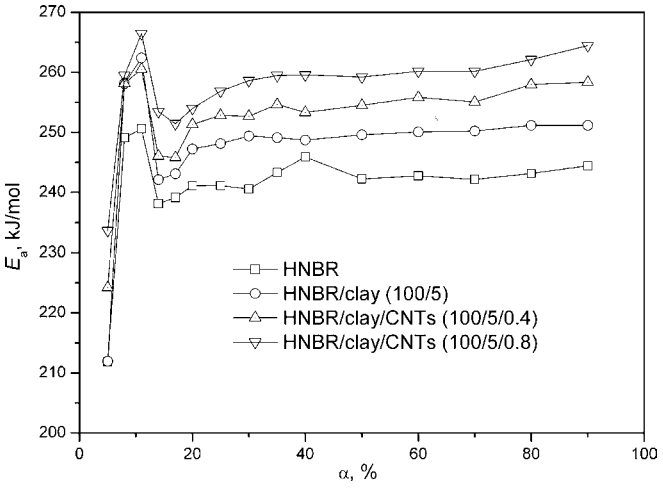

Fig. 4. Activation energies versus α obtained by Friedman method.

Table 4
Kinetic parameters of thermal degradation calculated by Friedman method.

HNBR/clay/CNTs	E_a (kJ/mol)	n
100/0/0	243	1.1
100/5/0	250	1.3
100/5/0.4	254	1.3
100/5/0.8	259	1.4

loss appears, while the second part, where the substantial mass loss takes place, is due to the main degradation mechanism. The differences of E_a on α between Friedman and Flynn–Wall–Ozawa methods indicate the Friedman method is more sensitive than Flynn–Wall–Ozawa method in the low α area. The difference of the calculated E_a by two methods can be explained by a systematic error due to improper integration [9]. The Friedman method employs instantaneous rate values being, therefore, it become sensitive to experimental data. The equation of Flynn–Wall–Ozawa method is derived assuming a constant E_a, introducing systematic error in the estimation of E_a in the case that E_a varies with α. An error can be estimated by comparison with the Friedman method results [34].

The thermal degradation of HNBR can be considered to a reaction between 1-order and 2-order, while the addition of clay or CNTs increases the n slightly, indicating the thermal degradation mechanism becomes complicatedly [33]. The degradation kinetics of HNBR inclines to under diffusion control and thus the observed kinetic parameters increase, as clay and CNTs act as a char promoter slowing down the degradation and providing a protective barrier to prevent the diffusion of degradation products [35].

It can also be seen that although there is a big discrepancy on the value for various samples between Friedman method and Kissinger method, both methods have obtained the same E_a order just mentioned above. Budrugeac et al. [36] evaluated the validity of non-isothermal kinetics methods used to calculate the E_a, The Flynn–Wall–Ozawa and Friedman methods give results that agree with each other only if the E_a does not change with the conversion degree [36]. In this work, the result calculated by Flynn–Wall–Ozawa method shows the E_a is independent with the conversion degree, it could be concluded that the results of the above three methods are consistent with each other and reliable.

3.4. TGA-FTIR

Time-resolved FTIR spectra during degradation process of HNBR nanocomposites in nitrogen atmosphere are shown in Fig. 5 and the *in situ* FTIR spectra of degradation products at each weight loss are shown in Fig. 6. The remarkable absorption peaks of hydrocarbons appear when α is 10%. The peaks at 2860 and 2930 cm^{-1} are assigned to the symmetrical and asymmetrical deformation vibration of CH_2. The peaks at 1460 and 1650 cm^{-1} correspond to the C–H deformation vibration and double bond, respectively. There are no peaks of CH_3 in 2870 and 2960 cm^{-1} of deformation vibration and in 1375 cm^{-1} of bending vibration. Fuh and Wang [37] found 1,3-butadiene and acetonitrile are the degradation products of nitrile-butadiene rubber by using pyrolysis/gas chromatography/mass spectrometry. Double bond migration followed by allylic cleavage results in the formation of propene and acetonitrile. So it can be concluded that the main degradation products are olefins with end group of double bond or acetonitrile. Fig. 5 shows that the peak at 1460 cm^{-1} in HNBR/clay/CNTs is lower than that in HNBR/clay and Fig. 6 shows the HNBR/clay/CNTs nanocomposites spent more time than HNBR/clay to reach the same α, indicating that the clay-CNTs filler network reduced the diffusion speed of degradation products [21]. There are no obvious peaks before 2000 s in HNBR/clay/MWNTs composite, while such peaks appear before 2000 s in HNBR/clay composite (Fig. 5), indicating

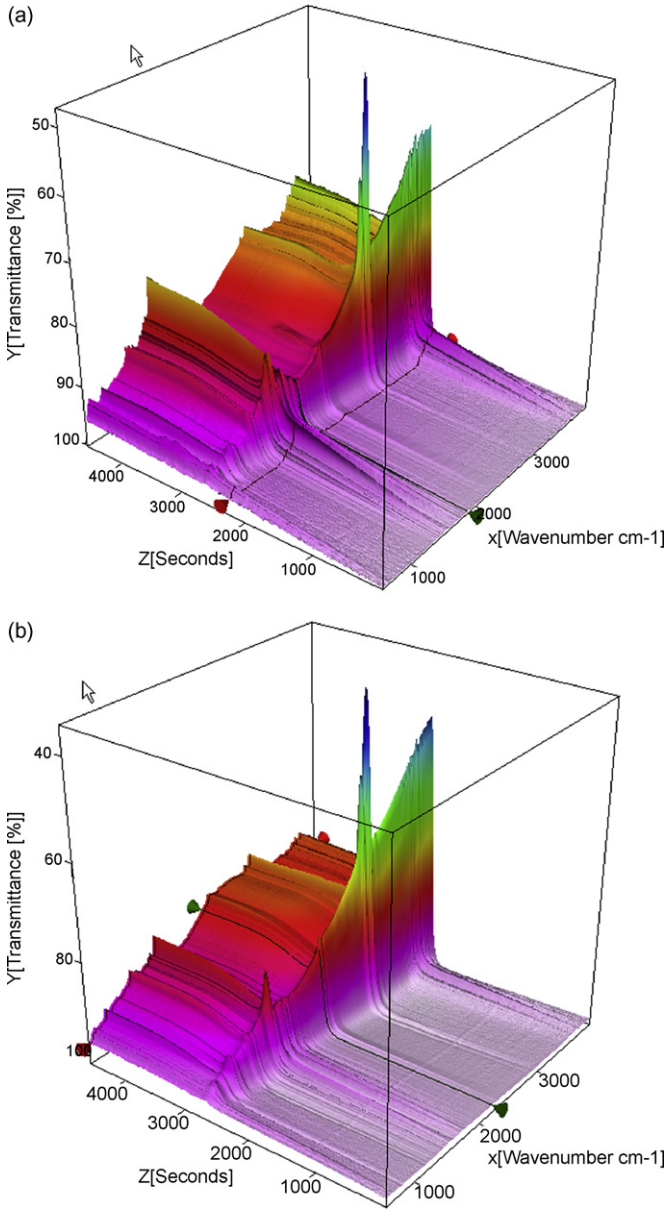

Fig. 5. Three-dimensional FTIR spectra corresponding to gases involved in the thermal degradation of HNBR composites (a) HNBR/clay (100/5), (b) HNBR/clay/CNTs (100/5/0.4).

HNBR/clay/MWNTs delays the decomposition time and has a high degradation temperature than HNBR/clay. At the same α (95%), the deformation vibration peak of CH_2 of HNBR/clay/CNTs is much lower than that of HNBR/clay, indicating that at high α, the thermal degradation of HNBR/clay/CNTs became slow, while the degradation reaction was still continue. This is probably due to the char layer of HNBR/clay/CNTs is more compact and effective in hindering molecule motion than that of HNBR/clay [21].

The results of the above three methods and TGA-IR reveal the role of clay and CNTs played in the HNBR matrix: when HNBR/clay or HNBR/clay/CNTs nanocomposites were heated to decompose, the involved clay gradually forms char layers to separate the underlying matrix, preventing the HNBR matrix from further degradation [19], hence leading to the increase of E_a of HNBR. The addition of CNTs cooperates with clay to form more complete charred layers [22] and has a more strongly inhibitive effect on the degradation, causing reducing the diffusion speed of degradation products and further increasing of thermal degradation E_a of HNBR.

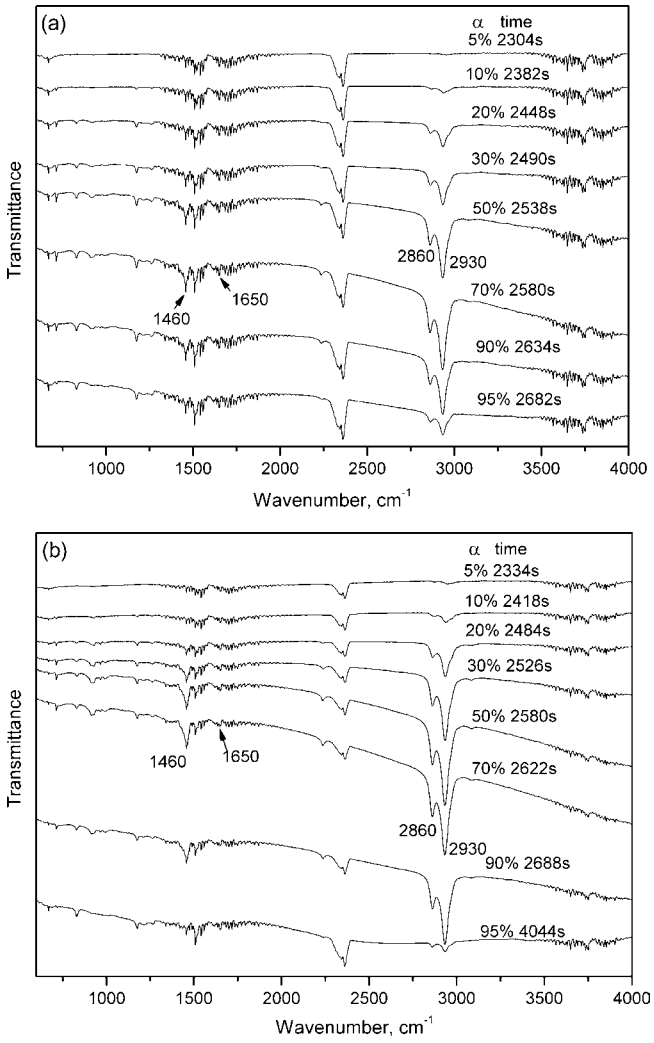

Fig. 6. TGA-FTIR spectra at different α for HNBR (a) HNBR/clay, (b) HNBR/clay/CNTs (100/5/0.4).

3.5. Conclusions

The initial degradation temperature (temperature at weight loss of 5 wt%) sequence of hydrogenated nitrile-butadiene rubber (HNBR) and its nanocomposites is HNBR/clay/CNTs > HNBR/clay > HNBR. The analysis of thermal degradation kinetic parameters of HNBR and HNBR nanocomposites calculated using Kissinger, Flynn–Wall–Ozawa and Friedman methods showed that the activation energy (E_a) increased after the addition of clay and CNTs, especially the small amount of CNTs could increase the E_a of HNBR/clay nanocomposites, which can be ascribed to the better thermal stability of the char layer formed with good barrier property as the interaction between clay and CNTs. Clay and CNTs do not change the reaction mechanism of thermal degradation. The main thermal degradation products of HNBR are olefins with end group of double bond or acetonitrile and the clay-CNTs filler network reduced the diffusion speed of degradation products.

Appendix A

R	Gas constant = 8.3136 J/(mol K)
T	Absolute temperature (K)
α	Conversion degree
t	Reaction time (s)
β	Heating rate (K/min)
k	Rate constant associated with the temperature

References

[1] G. Severe, J.L. White, J. Appl. Polym. Sci. 95 (2005) 2–5.
[2] W. Zhao, L. Yu, X. Zhong, Y. Zhang, J. Sun, J. Appl. Polym. Sci. 54 (1994) 1199–1205.
[3] M. Giurginca, T. Zaharescu, Polymer 41 (2000) 7583–7587.
[4] K.G. Gatos, N.S. Sawanis, A.A. Apostolov, R. Thomann, J. Karger-Kocsis, Macromol. Mater. Eng. 289 (2004) 1079–1086.
[5] K.G. Gatos, L. Százdi, B. Pukánszky, J. Karger-Kocsis, Macromol. Rapid Commun. (2005) 915–919.
[6] X.G. Li, M.R. Huang, J. Appl. Polym. Sci. 71 (1999) 565–571.
[7] K. Chrissafis, K.M. Paraskevopoulos, S.Y. Stavrev, A. Docoslis, A. Vassiliou, D.N. Bikiaris, Thermochim. Acta 465 (2007) 6–17.
[8] K. Chrissafis, G. Antoniadis, K.M. Paraskevopoulos, A. Vassiliou, D.N. Bikiaris, Compos. Sci. Technol. 67 (2007) 2165–2174.
[9] V. Vladimirov, C. Betchev, A. Vassiliou, G. Papageorgiou, D. Bikiaris, Compos. Sci. Technol. 66 (2006) 2935–2944.
[10] S. Vyazovkin, N. Sbirrazzuoli, Macromol. Rapid Commun. 27 (2006) 1515–1532.
[11] S. Hirunpraditkoon, A.N. García, Thermochim. Acta 482 (2009) 30–38.
[12] E.C. Chen, T.M. Wu, Polym. Degrad. Stab. 92 (2007) 1009–1015.
[13] P. Potschke, B. Kretzschmar, A. Janke, Comp. Sci. Technol. 67 (2007) 855–860.
[14] T. Kashiwagi, E. Grulke, J. Hilding, R. Harris, W. Awad, J. Douglas, Macromol. Rapid Commun. 23 (2002) 761–765.
[15] D. Felhos, J. Karger-Kocsis, D. Xu, J. Appl. Polym. Sci. 108 (2008) 2840–2851.
[16] M. Maiti, S. Mitra, A.K. Bhowmick, Polym. Degrad. Stab. 93 (2008) 188–200.
[17] Q. Kong, Y. Hu, L. Song, Y. Wang, Z. Chen, W. Fan, Polym. Adv. Technol. 17 (2006) 463–467.
[18] J.W. Gilman, Appl. Clay. Sci. 15 (1999) 31–49.
[19] A. Huang, X. Wang, D. Jia, Y. Li, E-Polymers 28 (2007) 1–11.
[20] L. Liu, J.C. Grunlan, Adva. Func. Mater. 17 (2007) 2343–2348.
[21] H. Ma, L. Tong, Z. Xu, Z. Fang, Nanotechnology 18 (2007).
[22] F. Gao, G. Beyer, Q. Yuan, Polym. Degrad. Stab. 89 (2005) 559–564.
[23] G. Beyer, Polym. Adv. Technol. 17 (2006) 218–225.
[24] C. Tang, L. Xiang, J. Su, K. Wang, C. Yang, Q. Zhang, Q. Fu, J. Phys. Chem. B 112 (2008) 3876–3881.
[25] H.E. Kissinger, Anal. Chem. 29 (1957) 1702–1706.
[26] T. Ozawa, Bull. Chem. Soc. Jpn. 38 (1965) 1881–1886.
[27] H.L. Friedman, J. Macromol. Sci. Part A 1 (1967) 57–59.
[28] A.W. Coats, J.P. Redfern, Nature 201 (1964) 68–69.
[29] L. Núñez, F. Fraga, M.R. Núñez, M. Villanueva, Polymer 41 (2000) 4635–4641.
[30] G. Beyer, Fire Mater. 29 (2005) 61–69.
[31] G. Beyer, Fire Mater. 26 (2002) 291–293.
[32] J.D. Peterson, S. Vyazovkin, C.A. Wight, Macromol. Chem. Phys. 202 (2001) 775–784.
[33] Y. Chen, Q. Wang, Polym. Degrad. Stab. 92 (2007) 280–291.
[34] S. Vyazovkin, J. Comput. Chem. 22 (2001) 178–183.
[35] S. Bourbigot, J.W. Gilman, C.A. Wilkie, Polym. Degrad. Stab. 84 (2004) 483–492.
[36] P. Budrugeac, A.L. Petre, E. Segal, Therm. Anal. 47 (1996) 123–134.
[37] M-R.S. Fuh, G.Y. Wang, Anal. Chimica Acta 371 (1998) 89–96.